

Optical Engineering

OpticalEngineering.SPIEDigitalLibrary.org

Optical single-sideband modulation based on silicon-on-insulator coupled- resonator optical waveguides

Shijie Song
Xiaoke Yi
Suen Xin Chew
Liwei Li
Linh Nguyen
Rongkun Zheng

Optical single-sideband modulation based on silicon-on-insulator coupled-resonator optical waveguides

Shijie Song,^a Xiaoke Yi,^{a,*} Suen Xin Chew,^a Liwei Li,^a Linh Nguyen,^a and Rongkun Zheng^b

^aUniversity of Sydney, Faculty of Engineering and Information Technologies, School of Electrical and Information Engineering, Building J03, Sydney 2006, Australia

^bUniversity of Sydney, Faculty of Science, School of Physics, Sydney 2006, Australia

Abstract. We propose and demonstrate for the first time an optical single-sideband (OSSB) modulation generation based on silicon-on-insulator coupled-resonator optical waveguides (CROWs) capable of operating at wide bandwidth with enhanced sideband suppression. The optimum order of the CROW filter was synthesized based on comprehensive performance analysis including optical sideband suppression and electrical power variation. Experimental results demonstrate an OSSB signal with sideband suppression as large as 23 dB. The performance of the proposed OSSB was demonstrated via compensating radio frequency (RF) power degradation in the transmission of the RF signal within the fiber. © The Authors. Published by SPIE under a Creative Commons Attribution 3.0 Unported License. Distribution or reproduction of this work in whole or in part requires full attribution of the original publication, including its DOI. [DOI: [10.1117/1.OE.55.3.031114](https://doi.org/10.1117/1.OE.55.3.031114)]

Keywords: modulation; nanophotonics; ring resonator.

Paper 151060SS received Jul. 31, 2015; accepted for publication Sep. 18, 2015; published online Oct. 20, 2015.

1 Introduction

Microwave photonics, which brings together the worlds of radiofrequency engineering and optoelectronics, has led to an ever-increasing interest in its use for the generation, processing, control, and distribution of microwave and millimeter-wave signals.^{1–4} In microwave photonic systems, optical single-sideband (OSSB) modulation is often required for applications, such as radio-over-fiber transmission, photonic controlled phased array antenna, microwave photonic phase shifter, and optical vector network analyzer.^{5–8} Heretofore, various approaches have been presented to generate OSSB modulation. One method is by means of $\pi/2$ -phase shift via hybrid coupler in a dual-input Mach–Zehnder modulator or polarization modulator^{9,10} or via optical Hilbert transformer.^{11,12} A design with an optical fiber Sagnac loop and dual-electrode traveling wave modulator was also demonstrated to achieve OSSB modulation where the modulated bandwidth was mainly limited by the hybrid radio frequency (RF) coupler.¹³ Another way to generate OSSB signals is based on the usage of optical filtering to eliminate one of the optical sidebands in an intensity modulation or phase modulation scheme. This has been demonstrated by different approaches, such as stimulated Brillouin scattering, uniform fiber grating notch filter, and phase shift fiber Bragg grating for narrow sideband selection.^{14–16} Recently, integrated microwave photonics devices based on ring resonator structures have been of great research interest in integrated photonics as they are small and exhibit excellent performance.^{17–19} In particular, OSSB has been achieved in Ref. 20 via the use of a ring resonator assisted Mach–Zehnder interferometer to suppress the optical sideband for RF signals between 1.2 and 2.2 GHz. A silicon ring modulator was used to modulate signal wavelengths located at the resonance null achieving OSSB signal generation at a single frequency of 60 GHz.²¹

Moreover, the high index contrast in the silicon-on-insulator (SOI) material makes it an attractive platform for compact coupled-resonator optical waveguides (CROWs),²² offering the significant advantage of cascading monolithically with other silicon photonic modulators, such as those demonstrated in Ref. 23. Although SOI CROW filters have been used in various functions such as wavelength division multiplexing channelizers and multiplexers due to their favorable characteristics as highly selective filters and optical delay lines due to the large group delay near resonance,^{24,25} their application in OSSB modulation systems has not been investigated. In fact, the flexible synthesis platform of CROW, which facilitates the design of high-order optical filters with a flat-top response at the passband, provides a captivating profile for high sideband suppression over a wide range of microwave frequencies.

In this paper, we propose and demonstrate a novel OSSB modulation generation based on a compact high-order integrated SOI CROW filter. An analysis of different orders of CROW filters specifically for OSSB modulation is presented while including meticulous dissection of the impacts of both the amplitude and phase of the optical filters as well as RF power variations due to the fiber dispersion. In addition, we have also substantiated the use of an SOI CROW-based optical bandpass filter that features a wide and flat passband as well as a sharp rolloff to significantly increase the operating bandwidth of the OSSB modulation. Experimental results show an optimum OSSB modulation generation with sideband suppression over 23 dB and RF power ripple around ± 1 dB for wideband transmission of RF signals in a dispersive medium with a group delay slope of +330 ps/nm.

2 Simulation Results and Discussions

In the proposed OSSB modulation generation, a high-order bandpass filter based on CROWs is utilized to select the optical carrier and one of the sidebands of an optical double sideband (ODSB) signal. In order to facilitate a maximum

*Address all correspondence to: Xiaoke Yi, E-mail: xiaoke.yi@sydney.edu.au

suppression ratio, the carrier needs to be positioned close to the edge of the filter slope such that the unwanted sideband falls on the steep edge of the filter while the remaining sideband lies ideally within or close to the flat passband of the filter to prevent subsequent attenuation of the desired sideband. This leads to one sideband being significantly attenuated while the other is passed through relatively unaffected. Thus, the design of the high-order bandpass filter is a crucial aspect in optimizing the performance of the OSSB system and the goal is to determine the optimal parameters that satisfy the performance measures of the required OSSB modulation system. In this paper, the design specifications of the OSSB modulation system are: (i) large sideband suppression and (ii) small RF power variations via dispersive medium, e.g., optical fiber.

2.1 Sideband Suppression

First, we investigate the performance of various orders of SOI CROWs for OSSB modulation. A mode coupling method was used in the bandpass filter design.²⁶ A unified filter bandwidth of 70 GHz was considered in order to accommodate high-frequency RF signals. To maintain a small footprint size while still keeping the bending loss small, the ring radius was set as a value of about 4 μm .²⁷ Figure 1 shows the simulated amplitude and phase responses of CROW filters of different orders. As the order of the microring filter increases, the increase in the steepness of the phase slope and also the improved filter shape factor is clearly visible. Figure 2 shows the amount of sideband suppression ratio obtainable at microwave frequencies of about 10, 20, and 30 GHz for a fixed optical carrier with an operating wavelength positioned at the rising edge of the different orders of filters. As can be seen, the sixth-, seventh-, and eighth-order filters based on CROWs show an achievement of over 20-dB sideband suppression. The maximum rate of increase in sideband suppression occurs at the transition from the fifth to sixth order filter with more than a 5-dB increment observed. The subsequent increase in the order of filters from 6 to 8 will only increase the sideband suppression by 1-dB margin for every additional microring introduced.

2.2 Radio Frequency Power Variations

Next, we analyze the RF responses of the resulting OSSB modulation generation after propagating across a dispersive medium. Different lengths of single-mode fibers were considered in the simulation in order to fully comprehend

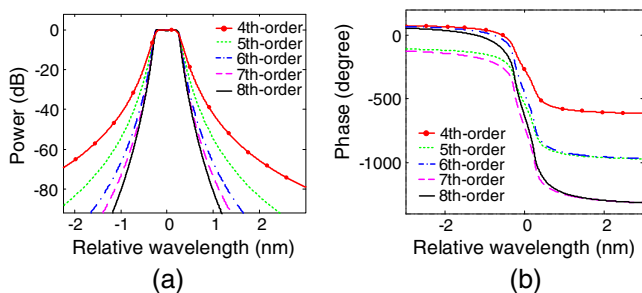


Fig. 1 (a) Transmission and (b) phase responses of different orders of bandpass filters-based coupled-resonator optical waveguides (CROWs).

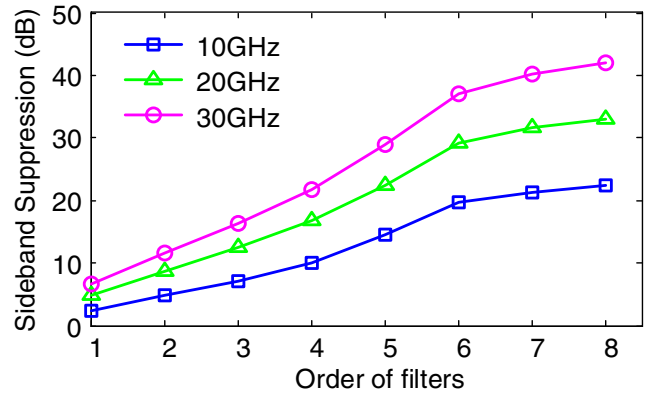


Fig. 2 Sideband suppression ratio as a function of the order of filters at microwave frequencies of 10, 20, and 30 GHz.

the performance of the proposed OSSB modulation. Moreover, each of the CROW filters intrinsically presents an additional optical phase shift to the system, where their phase responses can be seen in Fig. 1(b). Since this will introduce an added frequency-dependent phase change to the remaining sidebands and carrier, it is necessary to investigate the optical phase effects of CROW bandpass filters of different orders on the detected RF responses. Figure 3 shows the RF power fluctuations of the received OSSB signal after transmitting via different fiber lengths with and without considering the influence of the CROW filter phase. To maximize the operating bandwidth of the OSSB modulation, the carrier was placed at the location that contributed to the least amount of RF power ripple, which is close to the 3-dB point of the filter response. A typical dispersion value of 17 ps/nm/km for a standard single-mode fiber at 1550 nm and a RF bandwidth from 40 MHz to 40 GHz for the OSSB modulation was used in the simulation. It can be seen that the effect of the optical filter phase generates a slight increase of about 0.3 and 0.5 dB in the overall RF variation for the fourth- and fifth-order filters, showing that the phase of the filter has a small impact on the RF power variations. The phase effect is even negligible in higher order CROW filters with sixth, seventh, and eighth orders, demonstrating an inconsequential effect on the received RF signal due to the linearity of the optical phase. For a fourth- and fifth-order microring CROW filter,

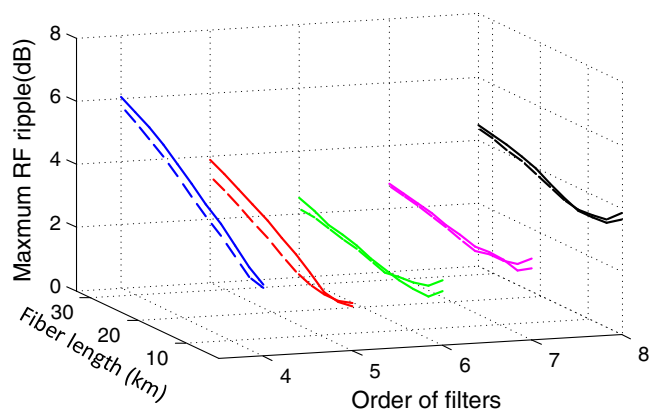


Fig. 3 Radio frequency (RF) power variation versus dispersion for microring CROW filters of various orders. Solid line: filter with phase. Dashed line: filter with zero phase.

it can be seen that the RF amplitude fluctuations increase rapidly with the increase of fiber lengths. This is primarily due to the low sideband suppression ratio, which allows dispersion to have dominating effects on the RF power variation. With the case of increased filter orders, the substantial increase in the sideband suppression ratio reduces the dependence of dispersion on the power ripple. This is evident by the fact that the variation in the obtained RF power with respect to the range of dispersion values analyzed is <2.5 and 2.7 dB for the sixth- and seventh-order filters, which is significantly smaller than the 6.1- and 3.8-dB increase in RF power variation obtained from the fourth- and fifth-order filters, respectively. However, despite the slightly higher suppression ratio displayed by the eighth-order filter at 10, 20, and 30 GHz, a distinctly higher RF power variation of 4.5 dB in the received signal was also observed indicating a possible compromise in the OSSB suppression ratio of lower frequency components for higher order filters. This is because apart from removing the unwanted lower sideband by positioning the carrier wavelength at the rising edge of the filter, it is to be noted that higher order filters will also introduce a consequent attenuation to the remaining optical sideband at low RF modulation frequencies due to the steep slope of the filter edge, thus leading to higher RF power variations. For an OSSB modulation with an operating RF bandwidth from 40 MHz to 40 GHz, the sixth-order filter provides the

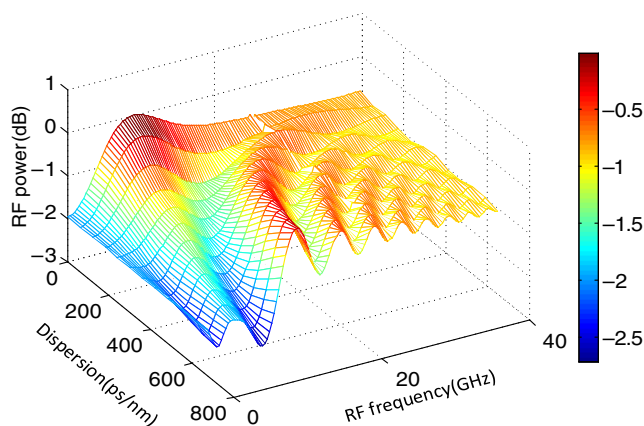


Fig. 4 RF power response as a function of dispersion parameter for optical single-sideband (OSSB) modulation generation based on sixth-order CROW filter.

optimized performance as it not only suppresses unwanted sidebands sufficiently but also minimizes the attenuation introduced to the remaining sidebands at low frequencies. This is apparent from the RF responses, as shown in Fig. 4, calculated at different levels of dispersion ranging from 0 to 600 ps/nm for the OSSB modulation generation based on a sixth-order CROW filter. It can be seen that although larger RF power variations are observable principally at low frequencies, the RF power ripples do not exceed 2.5 dB for the whole range of dispersion and RF frequency measured.

3 Experimental Results

Figure 5 shows the scanning electron microscope image of the sixth-order CROW filter fabricated on an SOI wafer, which is comprised of six weakly coupled resonators. The height of the silicon core waveguide is 220 nm and the width is 450 nm for both the bus and racetracks. The round trip length of each ring resonator is about 25 μm . To obtain a bus-ring power coupling coefficient of 0.25, the gap spacing between the bus waveguide and the racetrack ring resonator is 158 nm. To measure the amplitude response of the filter, a tunable laser source was externally controlled to sweep all wavelengths between 1553 and 1556 nm with a wavelength resolution of 10 pm. The measured optical response is obtained by monitoring the corresponding optical power change via an optical power meter. The phase response of the filter can be computed based on the measured group delay of the optical filter obtained using a modulation phase shift technique. For this measurement, the problem of phase ambiguity induced by unbalanced sidebands is avoided by using an optical single sideband modulator consisting of a dual electrode Mach-Zehnder modulator and an electrical hybrid coupler (Marki Microwave).^{28–30} Due to the cutoff frequency of the quadrature hybrid coupler, an RF signal at 2.5 GHz was generated from the vector network analyzer (Agilent N5230A) and applied onto the optical single sideband modulator, where the electrical signal obtained after photodetection was fed back to the vector network analyzer for group delay measurement. Figure 6 illustrates the measured amplitude and phase responses in blue solid lines while displaying the theoretical responses in red dashed lines as a comparison. The rising and falling edge slopes of the amplitude response were measured to be 71.9 and 98.7 dB/nm, respectively. The measured optical bandwidth

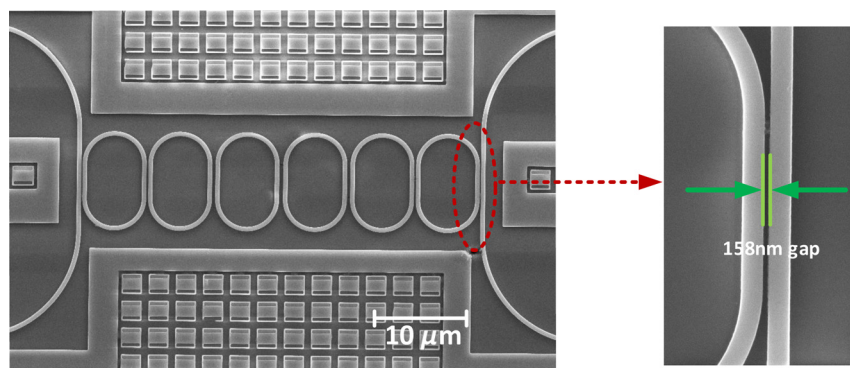


Fig. 5 Top-view scanning electron microscope image of the fabricated silicon-on-insulator microring CROW filter.

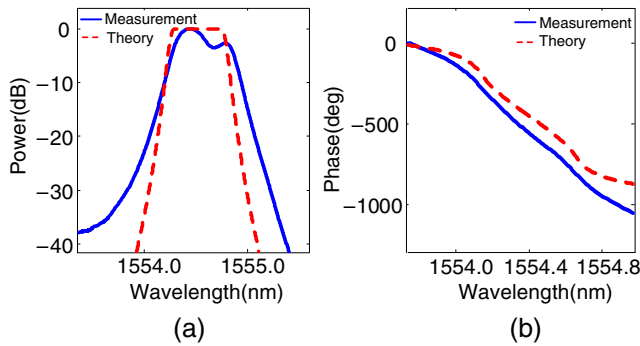


Fig. 6 Measured sixth-order CROW filter: (a) amplitude response and (b) phase response.

is about 70 GHz for the resonance located at 1554.5 nm. The filter passband shows a 3-dB deviation from the theoretical value, as depicted in Fig. 6(a), due to the inadvertent dimensional mismatch within the rings. This also has a direct implication on the plotted optical phase response, as shown in Fig. 6(b), which presents an offset and slightly enhanced nonlinearity in the accumulation of phase within the filter passband.

An experiment based on the setup shown in Fig. 7 was performed to verify the principle of the new OSSB generation system. A tunable laser source was modulated via an electro-optic modulator (EoSpace), driven by an RF oscillator (Agilent E8257D) that generates two optical sidebands before launching into the optical bandpass filter based on SOI CROWs. The fabricated filter suppresses one of the first order sidebands while the optical carrier and the other sidebands are passed through, thus achieving an OSSB modulation format. The resonance shift due to the temperature fluctuation is expected to be maintained within ± 0.2 GHz for a transverse electric waveguide mode with an effective index of 2.5 by using an external thermoelectric temperature controller (Newport) connected to the chip, which provides a thermal stability of ± 0.01 deg within 24 h.³¹ A linearly chirped fiber Bragg grating (LCFBG) was used to provide an optical dispersion identical to that of a 20-km single-mode fiber. Finally, the OSSB signal was received by the photodetector (u2t). As a proof of concept, Fig. 8 shows the optical spectra of the generated OSSB signal at 20 GHz measured by using a high resolution optical spectrum analyzer with a resolution bandwidth of 150 MHz (Finisar Wave Analyzer). The performances of the OSSB modulation with the suppression of lower and upper sidebands were investigated by considering two cases: where the optical carrier was first aligned at the rising edge, then followed by the falling edge of the filter. Utilizing first the rising edge of the filter, an OSSB signal with a lower sideband suppression of 20 dB was achieved when

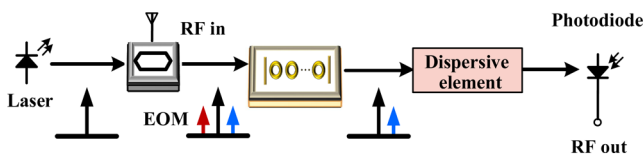


Fig. 7 Experimental setup of the single-sideband modulation system.

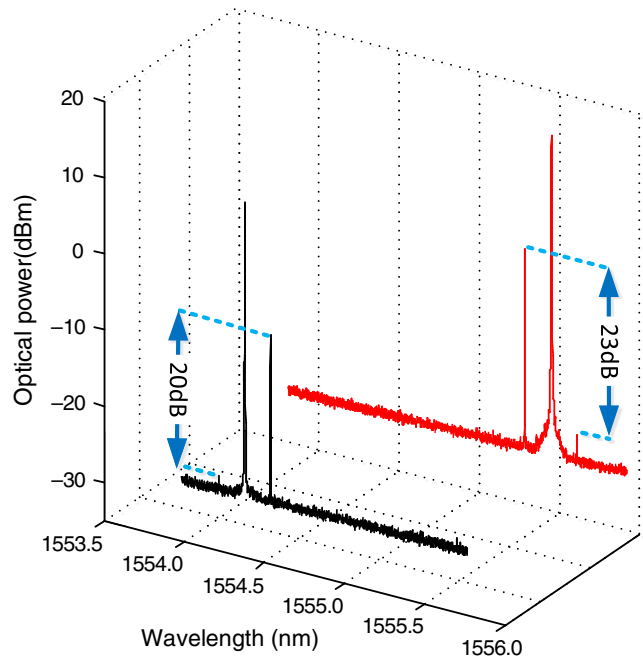


Fig. 8 Optical spectrum of the generated OSSB signal with lower sideband suppression (black line) and upper sideband suppression (red line) when modulated at 20 GHz (after passing through the optical filter).

the carrier wavelength was set to 1554.2 nm. When the carrier frequency was tuned to 1555.1 nm, the rising edge of the filter was deployed, thus converting the suppressed sideband from the lower sideband to the upper sideband and presenting an upper sideband suppression of 23 dB, as shown in the red line in Fig. 8. Sideband suppression can be further improved via minimizing the optical deviation of the SOI filter by reducing the fabrication mismatches. It is to be noted that the achievable sideband suppression depends on the relative position of the carrier with respect to the filter response and is thus affected by laser wavelength drift. To ensure the robustness of the system, a feedback control circuit can be employed to stabilize the laser while the deviation in the position of the filter response can be corrected via a thermal tuning mechanism.

To evaluate the performance of the presented OSSB modulation system, the RF frequency responses with and without the optical filter were experimentally measured. Here, an LCFBG (Proximion) with a group delay slope of +330 ps/nm was employed as the dispersive delay line. The RF signal recovered at the photodiode was measured by a 20-GHz vector network analyzer (VNA, Agilent). Figure 9 illustrates the measured RF power as a function of frequency. It can be seen that a deep dispersion-induced power fading of 33.2 dB is generated in an ODSB system without the usage of an optical filter for an OSSB modulation generation. On the contrary, the integration of the SOI optical bandpass filter into the system allows the RF response to be nearly constant over a wide frequency range from 0 to 20 GHz limited by the measurement range of the VNA, with ripples of 3.5 and 2 dB detected when the optical carrier was positioned at the rising and falling edges of the filter, respectively. The demonstration can be further extended to encompass monolithic or hybrid integration of the

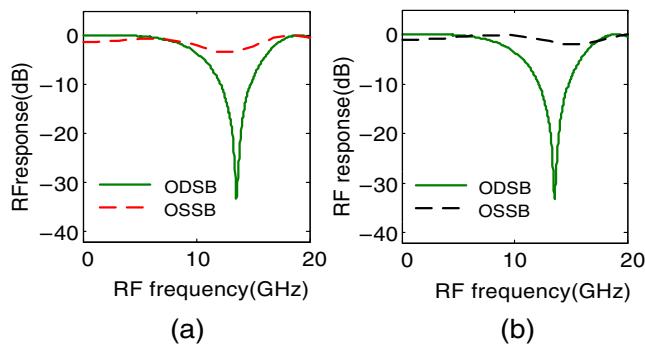


Fig. 9 RF responses of the ODSB and OSSB system with (a) upper sideband suppression (red dashed line) (b) lower sideband suppression (black dashed line).

electro-optic modulator and the CROW filter.²³ Current developments in integrated electro-optic modulators have already demonstrated a modulation bandwidth greater than 35 GHz based on carrier depletion, which makes integrated single-sideband modulation systems with large operating bandwidth possible in the near future.³²

4 Conclusion

In conclusion, we have proposed and experimentally demonstrated a novel OSSB modulation system by employing an optical bandpass filter based on SOI CROWs. To the best of our knowledge, this is the first experimental demonstration of using an SOI CROW filter to implement an OSSB modulation system capable of operating at a wide bandwidth with an effective suppression of the lower and upper sidebands. The measured RF power ripple of only 2 dB over a wide range is a strong indication that the system proposed is almost not affected by the fiber chromatic dispersion induced power penalty and is well suited to be implemented as a key component integrable in various microwave signal processing systems.

Acknowledgments

This work was supported by the Australian Department of Defence. The authors extend thanks to Pengju Bian and Jiangtao Qiu from University of Sydney for their help in SEM measurement.

References

1. R. A. Minasian, E. H. W. Chan, and X. Yi, "Microwave photonic signal processing," *Opt. Express* **21**(19), 22918–22936 (2013).
2. J. Capmany et al., "Microwave photonic signal processing," *J. Lightwave Technol.* **31**(4), 571–586 (2013).
3. T. Zhang et al., "High-spectral-efficiency photonic frequency down-conversion using optical frequency comb and SSB modulation," *IEEE Photonics J.* **5**(2), 7200307 (2013).
4. J. Liu et al., "Ultrahigh-Q microwave photonic filter with tunable Q value utilizing cascaded optical-electrical feedback loops," *Opt. Lett.* **38**(21), 4304–4307 (2013).
5. B. Ortega et al., "Variable delay line for phased-array antenna based on a chirped fiber grating," *IEEE Trans. Microwave Theory Technol.* **48**(8), 1352–1360 (2000).
6. Z. Tang, S. Pan, and J. Yao, "A high resolution optical vector network analyzer based on a wideband and wavelength-tunable optical single-sideband modulator," *Opt. Express* **20**(6), 6555–6560 (2012).
7. C. Wang and J. Yao, "Fiber Bragg gratings for microwave photonics subsystems," *Opt. Express* **21**(19), 22868–22884 (2013).
8. D. B. Adams and C. K. Madsen, "A novel broadband photonic RF phase shifter," *J. Lightwave Technol.* **26**(15), 2712–2717 (2008).
9. M. Xue, S. L. Pan, and Y. J. Zhao, "Optical single-sideband modulation based on a dual-drive MZM and a 120 hybrid coupler," *J. Lightwave Technol.* **32**(19), 3317–3323 (2014).

10. Y. M. Zhang, F. Z. Zhang, and S. L. Pan, "Optical single sideband modulation with tunable optical carrier-to-sideband ratio," *IEEE Photonics Technol. Lett.* **26**(7), 653–655 (2014).
11. C. Sima et al., "Phase controlled integrated interferometric single-sideband filter based on planar Bragg gratings implementing photonic Hilbert transform," *Opt. Lett.* **38**(5), 727–729 (2013).
12. Z. Li et al., "Optical single-sideband modulation using a fiber-Bragg-grating-based optical Hilbert transformer," *IEEE Photonics Technol. Lett.* **23**(9), 558–560 (2011).
13. M. Y. Frankel and R. D. Esman, "Optical single-sideband suppressed-carrier modulator for wide-band signal processing," *J. Lightwave Technol.* **16**(5), 859–863 (1998).
14. Y. Shen, X. Zhang, and K. Chen, "Optical single sideband modulation of 11-GHz RoF system using stimulated Brillouin scattering," *IEEE Photonics Technol. Lett.* **17**(6), 1277–1279 (2005).
15. J. Park, W. Sorin, and K. Lau, "Elimination of the fibre chromatic dispersion penalty on 1550 nm millimetre-wave optical transmission," *Electron. Lett.* **33**(6), 512–513 (1997).
16. S. R. Blais and J. Yao, "Optical single sideband modulation using an ultranarrow dual-transmission-band fiber Bragg grating," *IEEE Photonics Technol. Lett.* **18**(21), 2230–2232 (2006).
17. W. Bogaerts et al., "Silicon microring resonators," *Laser Photonics Rev.* **6**(1), 47–73 (2012).
18. J. F. Bauters et al., "Silicon on ultra-low-loss waveguide photonic integration platform," *Opt. Express* **21**(1), 544–555 (2013).
19. B. Guha, B. B. C. Kyotoku, and M. Lipson, "CMOS-compatible athermal silicon microring resonators," *Opt. Express* **18**(4), 3487–3493 (2010).
20. C. G. Roeloffzen et al., "Silicon nitride microwave photonic circuits," *Opt. Express* **21**(19), 22937–22961 (2013).
21. C. W. Chow et al., "Long-reach radio-over-fiber signal distribution using single-sideband signal generated by a silicon-modulator," *Opt. Express* **19**(12), 11312–11317 (2011).
22. F. Morichetti et al., "The first decade of coupled resonator optical waveguides: bringing slow light to applications," *Laser Photonics Rev.* **6**(1), 74–96 (2012).
23. G. T. Reed et al., "Silicon optical modulators," *Nature Photonics* **4**(8), 518–526 (2010).
24. A. Melloni et al., "Tunable delay lines in silicon photonics: coupled resonators and photonic crystals, a comparison," *IEEE Photonics Technol. Lett.* **2**(2), 181–194 (2010).
25. F. N. Xia et al., "Ultra-compact high order ring resonator filters using submicron silicon photonic wires for on-chip optical interconnects," *Opt. Express* **15**(19), 11934–11941 (2007).
26. H. C. Liu and A. Yariv, "Synthesis of high-order bandpass filters based on coupled-resonator optical waveguides (CROWs)," *Opt. Express* **19**(18), 17653–17668 (2011).
27. Y. Vlasov and S. McNab, "Losses in single-mode silicon-on-insulator strip waveguides and bends," *Opt. Express* **12**(8), 1622–1631 (2004).
28. R. Hui et al., "10 Gb/s SCM system using optical single side-band modulation," in *Proc. Optical Fiber Communication Conf.*, Anaheim (2001).
29. D. Derickson, Illustrated ed., *Fiber Optic Test and Measurement*, Prentice-Hall, New Jersey (1998).
30. T. Niemi, M. Uusimaa, and H. Ludvigsen, "Limitations of phase-shift method in measuring dense group delay ripple of fiber Bragg gratings," *IEEE Photonics Technol. Lett.* **13**(12), 1334–1336 (2001).
31. M. S. Nawrocka et al., "Tunable silicon microring resonator with wide free spectral range," *Appl. Phys. Lett.* **89**(7), 071110 (2006).
32. D. M. Gill et al., "Internal bandwidth equalization in a CMOS compatible Si-Ring modulator," *IEEE Photonics Technol. Lett.* **21**(4), 200–202 (2009).

Shijie Song received her BE degree in electronics and science from Shanghai University, Shanghai, China, in 2008, and her ME degree in electrical engineering from the University of Sydney, Sydney, Australia, in 2013. She is currently working toward her PhD in the Fibre-Optics and Photonics Laboratory, University of Sydney.

Xiaoke Yi received her PhD from Nanyang Technological University, Singapore, in 2004. Since 2003, she has been with the School of Electrical and Information Engineering, the University of Sydney, Australia. She is now an associate professor and also a QEII fellow awarded by the Australian research council. Her main research interests include photonic signal processing, microwave photonics, and phased-array antennas. She holds a number of patents granted and pending in these fields.

Suen Xin Chew received her BE degree in electrical engineering from the University of Sydney, Sydney, Australia, in 2013. She is currently

working toward her PhD in the Fibre-Optics and Photonics Laboratory, University of Sydney.

Liwei Li received the BE (Hons.) degree and PhD degree in electrical engineering, both from the University of Sydney, New South Wales, Australia, in 2009 and 2013 respectively. She is currently a research

postdoctoral in the School of Electrical and Information Engineering at the University of Sydney. Her current research focuses include microwave photonics, photonic signal processing, optical communication systems, lightwave technology and fibre-optic communications.

Biographies for the other authors are not available.